Cell Host & Microbe, Volume *30*

Supplemental information

Immunological memory to common cold coronaviruses assessed longitudinally over a three-year period pre-COVID19 pandemic

Esther Dawen Yu, Tara M. Narowski, Eric Wang, Emily Garrigan, Jose Mateus, April Frazier, Daniela Weiskopf, Alba Grifoni, Lakshmanane Premkumar, Ricardo da Silva Antunes, and Alessandro Sette

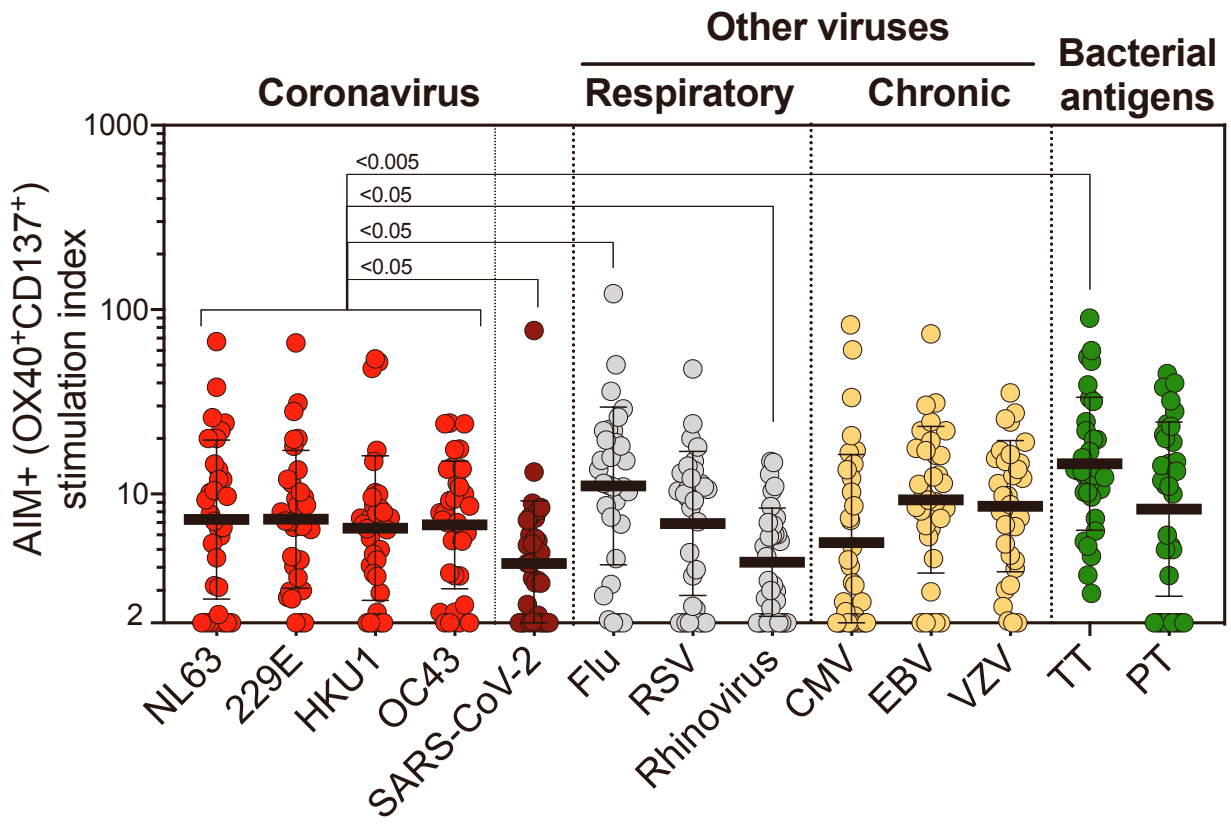

Figure S1. Stimulation Index of CD4+ T cell responses to four representative CCC and other pathogens, Related to Figure 1. Common cold coronavirus (CCC) and several other human pathogens-specific T cell responses were measured as percentage of AIM+ (OX40+CD137+) CD4+ T cells after stimulation of PBMCs with peptides pools. Graphs show individual response of the four CCC (NL63, 229E, HKU1, and OC43), SARS-CoV-2 and other pathogens plotted as stimulation index (SI) against DMSO negative control. First time point of the longitudinal series is plotted (n = 32). Data are represented as geometric mean and SD. Kruskal-Wallis test adjusted with Dunn's test for multiple comparisons was performed between the different antigens and each CCC viruses. Adjusted p values are shown for statistically significant comparisons ($p < 0.05$).

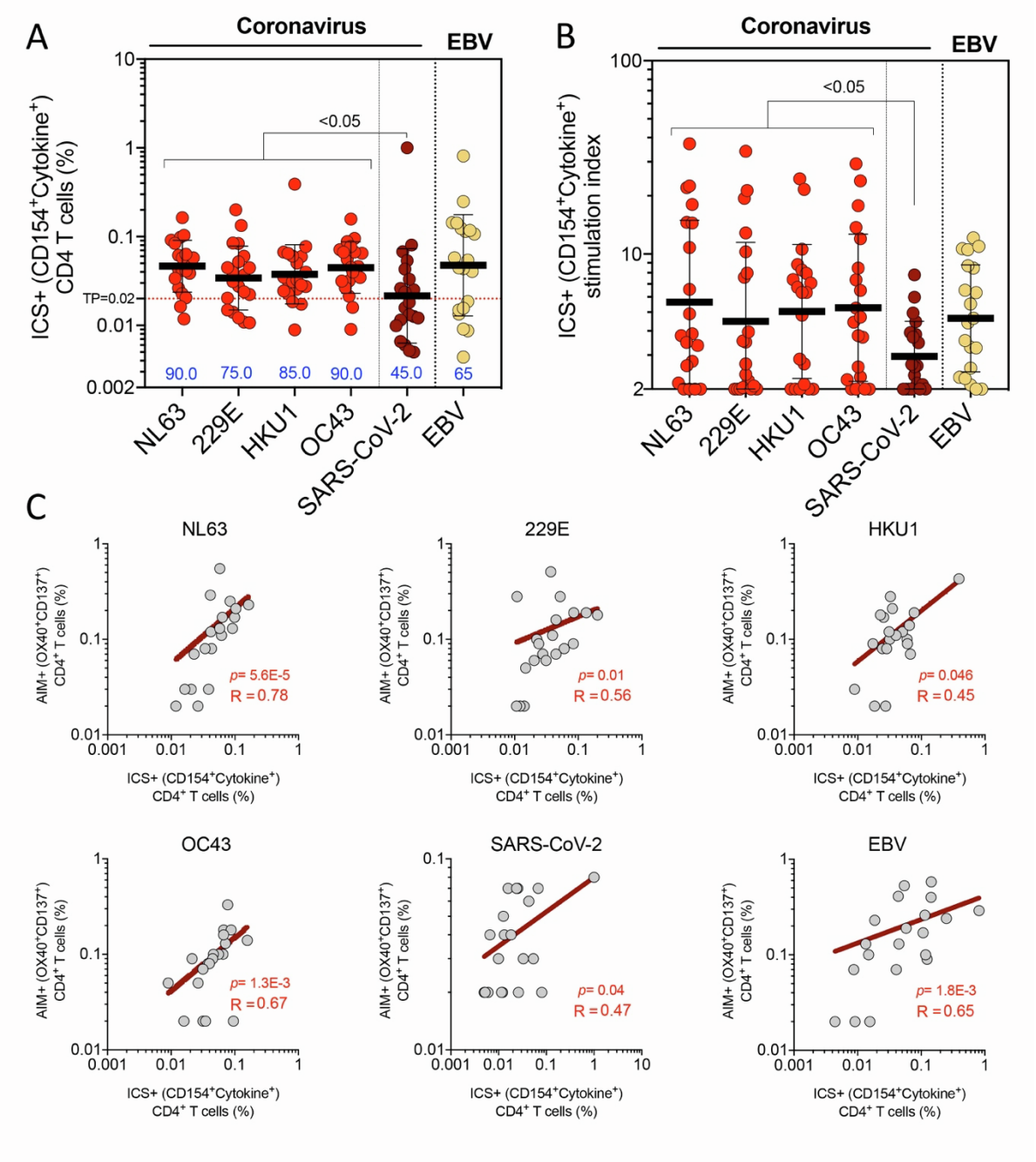

Figure S2. CCC-specific CD4+ T cell responses detected by ICS assay and correlation with AIM assay responses, Related to Figure 1. CD4+T cell cytokine responses (IFNγ, TNFα, IL-2, and Granzyme B) were measured by intracellular cytokine staining (ICS) of CD4+ T cells responding to antigen-specific stimulation as measured by CD154 (CD40L) expression. Graphs

show individual response of the four CCC (NL63, 229E, HKU1, and OC43), SARS-CoV-2 and EBV plotted as (**A**) total cytokine responses and (**B**) stimulation index (SI) against DMSO negative control. Donors from one of the time points of the longitudinal series are plotted (n = 20). Data are represented as geometric mean and SD. Kruskal-Wallis test adjusted with Dunn's test for multiple comparisons was performed between the different antigens and each CCC viruses. Adjusted p values are shown for statistically significant comparisons ($p < 0.05$). (**C**) Correlation of AIM+ (OX40+CD137+) CD4+ T cells responses and ICS+ (CD154+) CD4+T cell cytokine responses (IFNγ, TNFα, IL-2, and Granzyme B) were found after stimulation of PBMCs with four CCC, SARS-CoV-2 and EBV. Data from all 20 ICS study subjects were included and correlation were calculated by Spearman correlation test. P values < 0.05 were considered statistically significant.

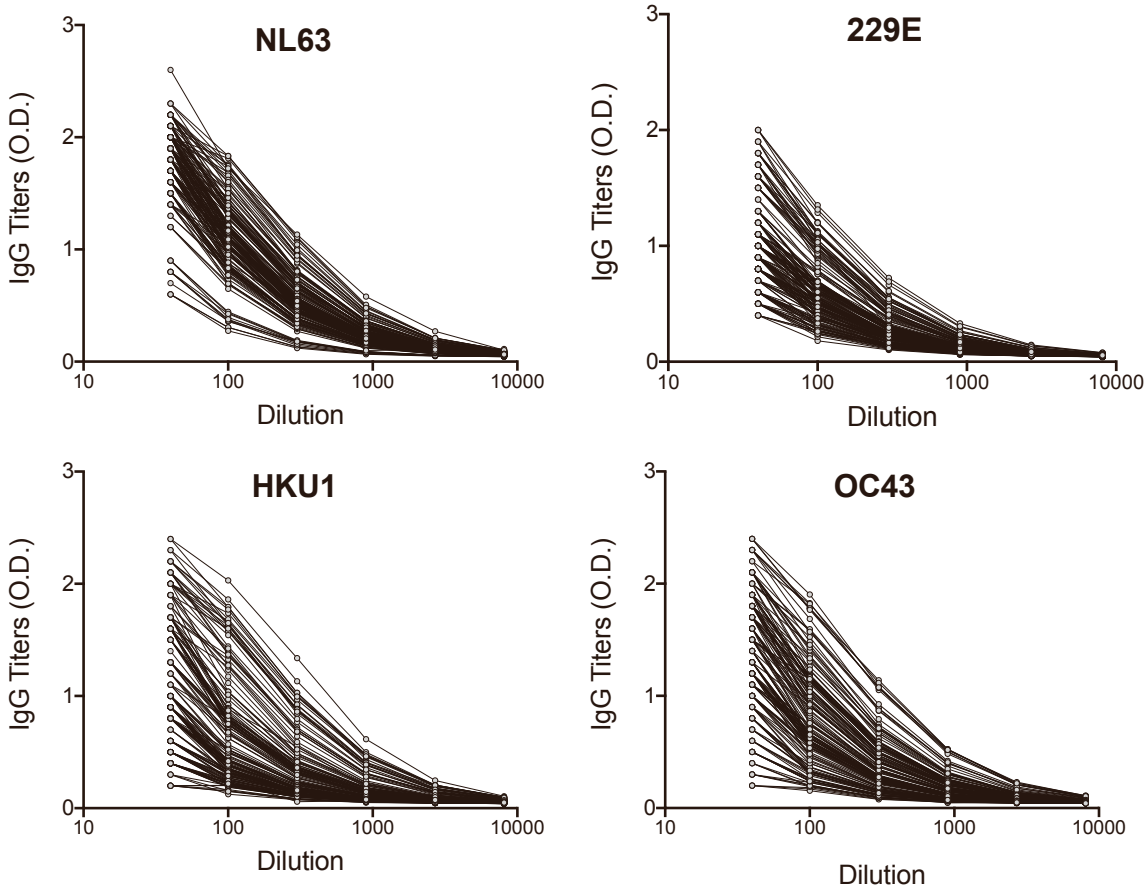

Figure S3. IgG serial dilutions for endpoint titers and AUC calculation, Related to Figure 5.

Plasma ELISA IgG serial dilutions to calculate the area under the curve (AUC) for CCC viruses (229E, NL63, HKU,1 and OC43) spike receptor binding domain (RBD) protein are shown for the longitudinal cohort (n = 32).

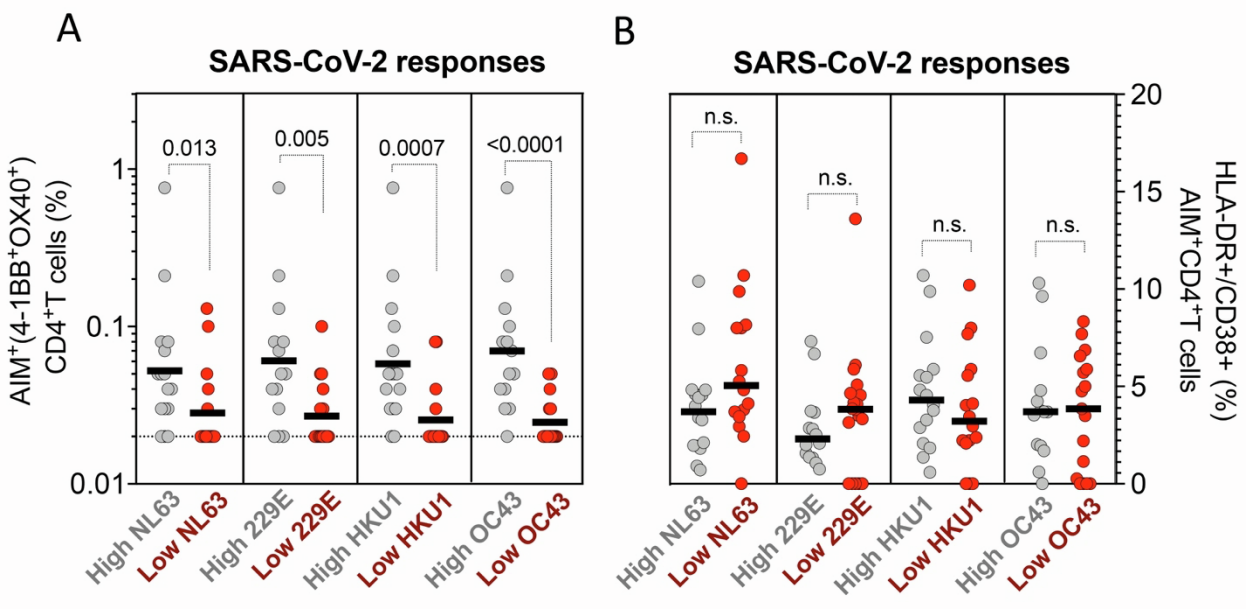

Figure S4. High CD4+ T cell reactivity across all the CCC viruses is associated with high pre-existing SARS-CoV-2 immunity, Related to Figure 6. (**A**) Antigen-specific T cell responses were measured as percentage of AIM+ (OX40+CD137+) CD4+ T cells after stimulation of PBMCs with peptides pools for CCC and SARS-CoV-2 (representing pre-existing immunity in pre-pandemic samples). (**B**) Recent activated CCC-specific T cell responses were measured by calculating the percent of HLA-DR$^+$CD38$^+$ of AIM+ (OX40$^+$CD137$^+$) CD4+ T cells. Each dot represents the response of an individual subject (n=32) at first time point. Median is shown. High responders for each CCC are shown in gray, and low responders in red. The different SARS-CoV-2 specific immune responses between high and low CCC responders were compared using Mann-whitney test, and p values < 0.05 considered statistically significant.

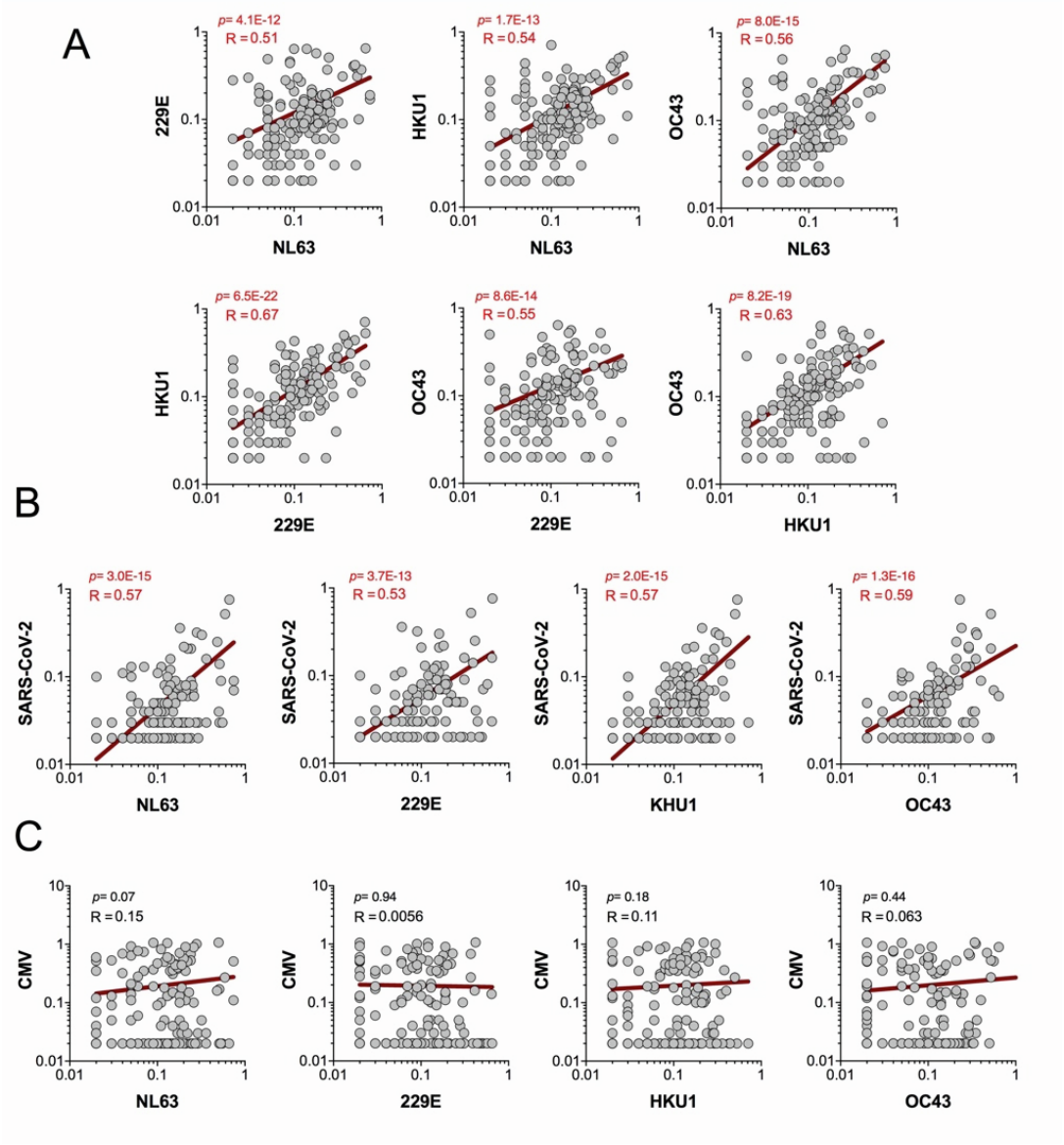

Figure S5. Correlation of CCC-specific CD4+ T cell responses among coronaviruses and SARS-CoV-2, Related to Figure 6. (**A**) Correlation of AIM+ CD4 T cell responses among common cold coronaviruses (CCC). (**B**) Correlation of AIM+ CD4 T cell responses between SARS-CoV-2 and all 4 CCCs. (**C**) No correlation of AIM+ CD4 T cell responses found between CMV and any of the 4 CCCs. Data from all visits of 32 study subjects were included and correlation were calculated by Spearman correlation test. P values < 0.05 were considered statistically significant.

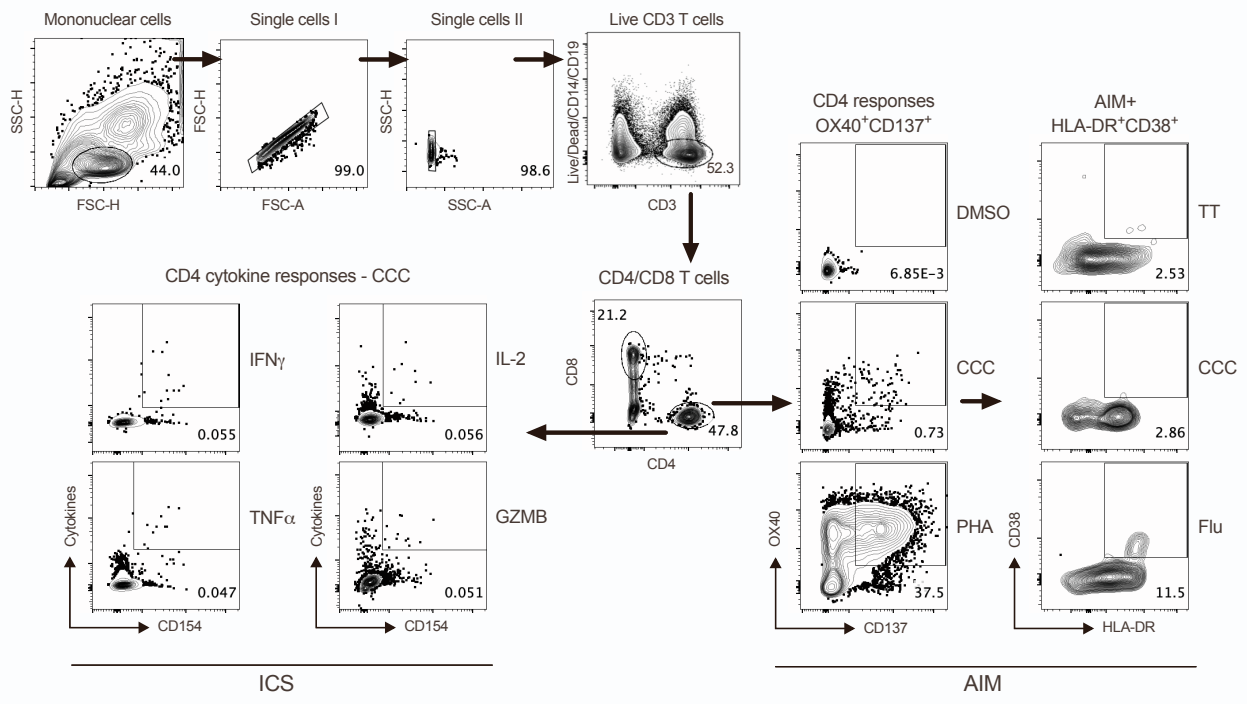

Figure S6. Illustrative flow cytometry gating strategy for the assessment of antigen-specific CD4+ T cell responses by AIM and ICS assays, Related to Figure 1 and 3. Representative gating of reactive OX40+CD137+ CD4+ T cells (AIM+) and CD4 cytokine responses (IFNγ, IL-2, TNFα and Granzyme B (GZMB)) from donor PBMCs is shown. Briefly, for both AIM and ICS, mononuclear cells were gated out of all events followed by subsequent singlet gating. Live CD3+ cells were gated as Live/Dead-CD14-CD19-CD3+. Cells were then gated as CD4+CD8-. For AIM, antigen-specific cells definied as OX40+CD137+ CD4+ T cells (AIM+) and after antigen stimulation, and frequencies calculated as percent of total CD4+ T cells. Representative AIM+ responses after stimulating with positive (PHA) or negative (DMSO) controls and CCC (OC43) specific megapools are presented on the right. Recently activated cells (HLA-DR+CD38+) were further gated from AIM+ cells. Representative plots are show for TT, CCC (OC43) and Flu. For ICS, antigen-specific cytoking producing CD4 T cells definied as Cytokine+ and CD154+ CD4 T cells and after antigen stimulation, and frequencies calculated as percent of total CD4 T cells. Representative ICS+ responses after stimulating with CCC (OC43) specific megapools are presented on the left.